CLM-P852

CLM-P852

Ion heating and power balance in the reversed field pinch

P.G.Carolan
A.Lazaros
M.G.Rusbridge
and
J.W.Long

UK ATOMIC ENERGY AUTHORITY

Culham Laboratory

Ion heating and power balance in the reversed field pinch

P G Carolan, A Lazaros+, M G Rusbridge* and J W Long°

Culham Laboratory, Abingdon, Oxon, OX14 3DB, UK
(UKAEA/Euratom Fusion Association)

+ Euratom Fellowship, Fusion Programme
* Physics Department, UMIST, Manchester
° Oxford Polytechnic

ABSTRACT

A power balance model of the RFP has been developed on the assumption that electrons are heated ohmically while the power associated with the fluctuations, $E \cdot j - \eta j^2$, is responsible for heating the ions. Anomalous diffusion due to turbulent convection is assumed to be the dominant loss mechanism for both ions and electrons and a single diffusion coefficient is used to describe both particle and energy losses. On making various assumptions of plasma behaviour, the model can account for the experimentally-observed diffusion coefficient, the ion and electron axial temperatures and radial profiles, as well as the scaling of electron temperature with density and current. The variation of the ratio of axial electron and ion temperatures with the insertion depth of the mobile limiter is HBTX1B is also quantitatively reproduced by the model.

Submitted to the 'Physical Review A'

INTRODUCTION

It is general finding in RFP's that ions are heated by non-collisional processes. This is clearly the case when T_i exceeds T_e [Carolan et al, 1987a; Wurden et al 1988]. For experiments where typically $T_{io} \sim T_{eo}$ [Bunting et al, 1985 and Carolan et al, 1988], collisional heating was also ruled out because the electron-ion equipartition time greatly exceeded the energy confinement time.

Another common observation in RFP's is that the total input power of the plasma ($\sim I_\phi V_\phi$ where I_ϕ is the toroidal current and V_ϕ the loop voltage) generally exceeds the total joule power ($=\int \eta_s j^2 d^3x$, where η_s is the Spitzer resistivity and j is the current density) by typically a factor of $\sim$2 to 3. This factor can be increased by the introduction of limiters into the plasma, or reduced by the removal of edge obstructions [Alper et al, 1988].

A clear association between the supra-joule power and ion temperature, at constant density, was found in the HBTX1B experiment. In other experiments [eg Wurden et al, 1988] where the electron density increases with plasma edge perturbation, the more general result is that the ratio T_{io}/T_{eo} increases with the loop voltage V_ϕ. Experimental observations thus provide a <u>prima facia</u> good case for ion heating being at least partly driven by the supra-joule input powers found in present RFP's.

In formulating an ion power balance model we make various assumptions which we attempt to check separately with experimental data. For example, the assumption made here that the ion and electrons are collisionally decoupled is generally found in experiment, given the observed T_i, T_e and n_e values. Other assumptions are more difficult to check experimentally, especially relating to spatial profiles and internal behaviour of, for example, the magnetic and fluid velocity fluctuations and how all of these depend on the plasma parameters. In such cases we attempt to show that the assumptions are at least internally consistent. We also allow the experimental results to guide the physics modelling; for instance, it is the ratio T_{io}/T_{eo} that is

most closely associated with the loop voltage, rather than T_{io} or T_{eo} separately, which suggests similar confinement physics for both particle species.

The approach here is to provide a general framework in modelling the ion power balance which proceeds from electrical measurements of plasma current, voltage, F and θ values to predictions of T_{io}/T_{eo}. ($F \equiv B_\phi(a)/[B_\phi]$, $\theta \equiv B_\theta(a)/[B_\phi]$ where $[B_\phi] = \int B_\phi(r)\, 2rdr/a^2$ and $B_\phi(a)$ and $B_\theta(a)$ are the edge values of the toroidal and poloidal magnetic fields). We propose solutions, or modelling, of the various elements in the framework but we do not claim that our choice of models is the only one justified by theory and experimental results. Since we get broad agreement between our model and many experimental results (eg. $T_i(r)$, T_e scaling with I_ϕ and n_e) then if it is shown that the modelling of a particular aspect is inadequate (eg. ion heating power modelling) there must be a corresponding correction to another element in the framework which can be further investigated.

The outline of the model is as follows (i) the electrons and ions are heated separately with, in most cases, only classical ohmic heating of the electrons (from $\eta_s j^2$) and the remaining power exciting fluid velocity fluctuations which heat the ions; (ii) both the ion and electron losses are dominated by convection with the same diffusion coefficient for both species and for both energy and particle transport; (iii) the relative diffusion coefficient is calculated from particle balance obtained from ionisation of the neutral particle density distribution as obtained from Monte-Carlo calculations; (iv) the diffusion coefficient on axis D(0) is obtained from electron power balance and from (iii) D(r) is obtained; (v) in calculating power losses we assume profiles of T_e, T_i and n_e remain substantially unchanged; (vi) plasma j and B profiles are calculated from external F and θ measurements using global helicity balance models and including finite β effects.

Several advances in the measurements of plasma parameters and in understanding of RFP physics now provide the basis for constructing an ion power balance model. Most important amongst these are:

(i) the observed increase in T_{io}/T_{eo}, with the insertion of a limiter in HBTX1B [Carolan et al, 1987a] and ZT-40M [Wurden et al, 1988], to values well in excess of unity; (ii) the reduction in T_{io}/T_{eo} below unity found in HBTX1B with the removal of the edge carbon tiles and its subsequent increase when the plasma is uncentred [Carolan et al, 1988]; (iii) the observation, first noted in HBTX1A [Carolan et al, 1985] and then more clearly shown in HBTX1B [Carolan et al, 1987b], that Z_{eff} was too low to account for the plasma resistance, even at relatively low values of I/N (5×10^{-14} A.m); the scaling of loop voltage with current on HBTX1B also reveals an anomalous voltage, ΔV_ϕ, which increased with limiter insertion and decreased with the removal of the edge limiter tiles, [Alper et al, 1988]; (iv) the incorporation of magnetic helicity loss at the plasma edge [Jarboe and Alper, 1987; Tsui, 1987] in helicity balance considerations offered an explanation for (iii); these treatments also revealed that only a small fraction of the power $I_\phi \Delta V_\phi$ ohmically heats the electrons; (v) the inclusion of finite pressure effects in the Modified Bessel Function Model (MBFM) [Johnston, 1981] significantly alters the λ-profile ($\lambda \equiv \mu_o a j_{||}/B$) [Ortolani, 1983] as deduced from the edge F and Θ values; (vi) the measurements of the T_i profile in HBTX1B [Field, 1988] and ZT-40M [Wurden et al, 1988] as inferred from Neutral Particle Analyser (NPA) measurements and more directly from fluorescent scattering [Forrest et al, 1988] and (vii) the measurements of the ion and impurity diffusion coefficients in HBTX1B [Carolan et al, 1987b].

Notwithstanding these developments, a physics account of the ion dynamics in an RFP plasma is still far from complete. Whilst there is a wealth of data available on axial measurements of T_i, T_e and Z_{eff}, and chord integrated electron densities, and global quantities such as the plasma resistance, only occasional profile measurements (e.g. $T_e(r)$) have been made in RFP plasmas.

The need to make several physics assumptions is therefore inevitable at this stage to obtain an ion power balance model which has predictive attributes rather than just a simple energy accounting of experimental results. While acknowledging the differences in the various RFP's (e.g. Z_{eff}) and the interpretation of the experimental

results we concentrate here on the HBTX1B experimental results and the previous physics descriptions that were advocated to explain them.

The experimental evidence for the contribution of non-collisional resistance and the non-collisional ion heating in the Reversed Field Pinch naturally led to considerations that these effects may be inter-related. Rusbridge (1969) was the first to assume that the link between these effects arise from the fluctuations in the magnetic and electric fields which may provide the ion heating and the resistance anomally. Here we incorporate more recent advances in the understanding of RFP's, as outlined above with several assumptions about the fundamental processes e.g. diffusion and heating.

In obtaining power balance we model separately the power input to, and the power loss from, the ions and the electrons, in a way consistent with the physics of the RFP (including recent theories on the helicity balance). Comparisons of predictions from the proposed power balance model are made with experimental results, particularly from the mobile limiter experiments and the plasma current scaling results. Finally, we suggest that non-collisional electron heating may become dominant at low values of ohmic heating i.e. low current and Spitzer resistivity.

INPUT POWERS

In RFP plasmas the coherence in the fluctuations of the magnetic field and fluid velocity are assumed to be important in maintaining the magnetic field configuration by dynamo action. Plasma relaxation is a continuous process in RFPs, so the associated fluctuations are always present. These fluctuations give rise to a dynamo electric field which must be included when deriving the current density distributions and the dissipated powers.

Ohm's law in the presence of fluid velocity fluctuations in a magnetized plasma is given by:

$$\underline{E} = \eta \underline{j} - \tilde{\underline{u}} \times \underline{B}, \qquad (1)$$

where η is the resistivity, $\underline{j}$ the current density, $\underline{B}$ the magnetic field and $\tilde{\underline{u}}$ the fluid velocity. The power input associated with Eqn.(1) is:

$$P_{tot} = \langle \underline{E}.\underline{j} \rangle = \langle \eta j^2 \rangle - \langle \tilde{\underline{u}} \times \underline{B}.\underline{j} \rangle, \qquad (2)$$

where $\langle \eta j^2 \rangle$ is the ohmic heating, P_Ω, which in the presence of the generally small current fluctuations, ($\underline{j} = \underline{j}_o + \tilde{\underline{j}}$) can be written as:

$$P_\Omega = \eta j_o^2 + \langle \eta \tilde{j}^2 \rangle \sim \eta j_o^2, \qquad (3)$$

The term $\langle \tilde{\underline{u}} \times \underline{B}.\underline{j} \rangle$ is the residual input power, P_f, associated with magnetic and velocity fluctuations, i.e.

$$P_f = \langle \underline{E}.\underline{j} \rangle - P_\Omega. \qquad (4)$$

In the presence of current and electric field fluctuations Eqn.(4) reduces to:

$$P_f = \langle \tilde{\underline{E}}.\tilde{\underline{j}} \rangle + E_\phi j_\phi - P_\Omega, \qquad (5)$$

where j_ϕ is the steady-state toroidal current and E_ϕ is the steady-state electric field i.e.

$$\langle E \rangle \equiv E_\phi = V_\phi / 2\pi R. \qquad (6)$$

It can be easily shown that $\langle \tilde{\underline{E}}.\tilde{\underline{j}} \rangle$ in Eqn(5) has no net contribution when integrated over the plasma volume. Here we assume that: $\langle \tilde{\underline{E}}.\tilde{\underline{j}} \rangle \ll E_\phi j_\phi$ (which may well be the case because $\tilde{j} \ll j_\phi$ and the time averaging effect), and so the residual power, P_f, takes the form:

$$P_f \sim E_\phi j_\phi - P_\Omega. \qquad (7)$$

Since the electron-ion equipartition time is much longer than the energy confinement time in present RFP plasmas [e.g. Carolan et al, 1987a], there is little energy transfer between the electrons and ions through collisions. Therefore, the two particle species can be treated

separately in power balance considerations. As we shall see later (cf. in particular the section dealing with the removal of tiles) the sharing of the local input power between electrons and ions may not be entirely straightforward but for the moment we assume that the electrons are heated ohmically by the current and the residual power input, p_f, is dissipated locally into the ions; the ion heating is discussed later. In these circumstances we can calculate the power input distributions for both the electrons and ions when the quantities involved in Eqns(3) and (7) (ie. η, $\underline{j}$ and E_ϕ) are determined.

The toroidal electric field, E_ϕ, is found from the measured values of V_ϕ. The magnetic field and current distributions in the so-called Modified Bessel Function Model, [Johnston, 1981] are obtained by an appropriate choice of the $\lambda(r)$ distribution ($\lambda(r) = \mu_o a j_{||}/B$) for which we assume a well behaved form: $\lambda(r)=\lambda(0)(1-(r/a)^\gamma)$, and by $\beta(0)$, ($\beta(0) \equiv 2\mu_o k\sum n(0)T(0)/B^2(0)$) which can be determined (for a particular $\lambda(r)$ distribution) from the experimental values of θ, F, β_θ. For HBTX1B, in particular, with the typical values of F=-0.07, θ=1.4 and β_θ=10%, the appropriate $\lambda(r)$ distribution is:

$$\lambda(r) = 2.7\ (1-(r/a)^{10}). \qquad (8)$$

Figure 1 shows that for θ=1.4, β_θ = 10%-20%, and the $\lambda(r)$ distribution of Eqn(8), $\beta(0)$ ranges from 3%-8%.

To estimate the resistivity, η, we include the constraint that the global magnetic helicity can be considered to be an invariant in sustained RFP plasmas. It has been suggested, [Jarboe and Alper, 1987] that the toroidal loop voltage can be regarded as having two components viz:

$$V_\phi = V_p + \Delta V_\phi, \qquad (9)$$

where ΔV_ϕ is the anomalous voltage arising from either the helicity dissipation in the edge region of plasma, or helicity loss from electrostatic fields at the boundary which have a component parallel to the local $\underline{B}$, [Tsui, 1987]. Both models are supported by the observed changes in the loop voltage required to sustain the current when the

edge conditions are altered (by limiter insertion or removal of the edge tile limiters), although the F, θ and Sptizer resistance, remain largely unaltered [Alper et al, 1988]. Here we associate V_p with the plasma volume, and given by:

$$V_p = \frac{1}{\Phi} \int \eta \, \underline{j}.\underline{B} \, d^3x, \tag{10}$$

[Schoenberg et al, 1984]. The value of $V_p = 13 \pm 2$ volts was obtained for $I_\phi = 200$ kA at the HBTX1B from:

$$V_p = I_\phi \Omega_p,$$

(where $\Omega_p \sim 65\mu$ Ohm is the plasma resistance in the absence of edge helicity disipation; Alper et al, 1988). The expression for the resistivity on axis obtained by Eqn (10) [Tsui et al, 1986] is:

$$\eta(0) = f_1 \, f_2 \, \frac{V_p}{I_\phi} \frac{a^2}{2R}, \tag{11}$$

where

$$f_1 = \frac{[B_\phi][j_\phi]}{[\underline{j}.\underline{B}]} \tag{12}$$

and

$$f_2 = \frac{[\underline{j}.\underline{B}]}{[\underline{j}.\underline{B} \; \eta(r)/\eta(0)]}, \tag{13}$$

and where [] denotes minor cross-sectional averaging. The profile form factors f_1 and f_2 depend on $\lambda(r)$, θ, β_θ (which determine $\underline{B}$, $\underline{j}$) and the resistivity, $\eta(r)$, whose relative distribution is given by:

$$\eta(r)/\eta(0) = (T_e(r)/T_e(0))^{-3/2}, \tag{14}$$

assuming Spitzer resistivity and a uniform Z_{eff}.

Other profile factors of interest are

$$f_3 = \frac{j_\phi(0)}{[j_\phi]} \tag{15}$$

and

$$f_4 = \frac{B_\phi(0)}{[B_\phi]}. \tag{16}$$

The distributions of j(r) and B(r) can be obtained from the relative distributions by setting:

$$j(0) = f_3 I_\phi/(\pi a^2) \quad \text{and} \quad B(0) = (f_4/\theta)(\mu_0 I_\phi/2\pi a).$$

For most operating conditions in HBTX1B, both with and without the edge tiles in position, the values of the profile factors are: $f_1 = 0.30$, $f_2 \approx 0.61$, $f_3 \approx 2.64$, $f_4 \approx 2.76$. The approximate constancy of these factors with plasma current arises because the λ profile is almost independent of the current for the data used here and where changes in F, θ relationship were mostly due to the variation of β_θ with current.

Distributions of the ohmic and residual input powers are shown in Fig. 2, for the following typical conditions of HBTX1B: $I_\phi = 200$kA, $V_\phi = 30$Volts, $V_p = 14$Volts, $F = -0.07$, $\theta = 1.4$, $\beta_\theta = 10\%$, $T_e(r) = T_{eo}(1-(r/a)^5)$, $T_{eo} = 250$eV, $n(r) = n_o(1-(r/a)^2)$, $n_o = 3.10^{19}m^{-3}$, and 156 tile limiters at the edge of plasma (covering 10% of the liner wall).

A noteworthy feature of the power input distributions of Fig. 2, as observed by others [e.g. Ortolani, 1984 and Schaffer, 1984], is the negative residual power in the outer region. In a fully relaxed Taylor state [Taylor, 1974], where $\lambda(r)$ is uniform, the volume integral of the residual power is identically zero. For the nonuniform $\lambda(r)$ profiles, (found experimentally in RFPs), the volume integral of the residual power is positive and of the same order to the ohmic power. It has been suggested [Tsui and Evans, 1988] that this negative residual power in the outer region is due to electromagnetic power transmission to the

inside, which extracts energy from the fluid motions. Alternatively it might be suggested that the power for the turbulence in the outer region is being supplied by the ions.

POWER LOSSES

In a sustained discharge the production of ions and electrons by ionisation of neutrals (originating from the wall), is balanced by the plasma loss by diffusion across the magnetic field. The particle balance equation in cylindrical symmetry has the form:

$$-\frac{1}{r}\frac{d}{dr}\,rG_p(r) = s(r), \qquad (17)$$

where $s(r)$ is the local ionisation rate and $G_p(r)$ the local particle flux. A turbulent convection model for the anomalous diffusion in the RFP, [Rusbridge, 1969] assumes "turbulent elements" of characteristic size $\Lambda_\perp$ transverse to the magnetic field and $\Lambda_{||}$ along it, which form from the background plasma, are convected through an average distance equal to $\Lambda_\perp$ with average speed $\tilde{u}_r$ before merging again with the background plasma. We identify $\Lambda_{||}$ and $\Lambda_\perp$ with the observed characteristic scale lengths of the magnetic field fluctuations and $\tilde{u}_r$ is determined from the measured electric field fluctuations. From this model a diffusion coefficient $D \sim \tilde{u}_r\,\Lambda_\perp$ can be obtained (which with the estimated values of $u_r \sim 2.10^3 m\ sec^{-1}$ and $\Lambda_\perp = 2.5cm$, gives $D \sim 50 m^2\ sec^{-1}$ which is the estimated value on axis for HBTX1B), but it is important to realise that the diffusing elements are flux tubes rather than individual particles; as a result the particle flux is given by:

$$G_p = -\frac{D}{V}\frac{d}{dr}\,(nV), \qquad (18)$$

where V, the volume of a unit flux tube, is an increasing function of radius ($V \propto B^{-1}$). The strength of this model is that it provides a natural explanation of the observed (approximately parabolic) density distribution when it is assumed that the plasma source (ionisation of neutrals) in concentrated near the wall; for, Eqn(17), allows a

solution nV = constant where $s(r) = 0$ so that $n(r)$ may be a decreasing function of radius. A more recent investigation, however, of the neutral density, both measured [Evans et al, 1984] and simulated by a Monte-Carlo treatment [Hughes and Post, 1978], has shown that the parabolic density profile admits an alternative explanation when substantial refuelling occurs in the plasma core. For these reasons, and because a closer examination shows that the idea of freely convecting flux-tubes cannot be sustained in a strongly sheared configuration, [S Gee, 1988] we shall use the simple classical form of Fick's Law, and the main assumption of the present work is that the same diffusion coefficient can be used for both the particle and energy transport, i.e.

$$G_p = -D(r)\,\frac{dn}{dr} \qquad \text{for the particles} \qquad (19a)$$

$$G_E = -D(r)\,\frac{dU}{dr} \qquad \text{for the energy} \qquad (19b)$$

where $D(r)$ is the diffusion coefficient and $U(r)$ is the energy density distribution ($= \frac{3}{2}\,nkT$). We emphasise that Eqns(19) are assumptions to be tested for consistency with the experimental results; we do not <u>a priori</u> exclude alternative loss processes, particularly for the electrons (such as thermal conduction along the field lines), but we shall show that no compelling evidence requires their inclusion.

Strictly speaking, Eqns(19) should include terms the nv_r and Uv_r on the r.h.s., representing the flux due to the inward 'pinching velocity' $v_r = -E_\phi B_\theta / B^2$. It is not difficult to show, however, that this velocity is of the order of a/τ_R where τ_R is the resistive diffusion time and since the actual confinement time is much shorter than this, the flux is correspondingly greater and the pinching term is negligible. In a typical case, the inclusion of the pinching term in the particle balance equation has been found to make only a 5% difference to the central density.

Equation (17), with the flux term given by Eqn(19a) can be written as:

$$-\frac{1}{r}\frac{d}{dr}\{r\,D(r)\,\frac{d}{dr}\,n(r)\} = s(r). \qquad (20)$$

In the same way when the power loss from the ions is assumed to be dominated by diffusion the ion power balance has the form:

$$-\frac{1}{r}\frac{d}{dr}\{r\,D(r)\,\frac{d}{dr}\,U_i(r)\} = p_f(r). \qquad (21)$$

Equation (20) can be used to provide the distribution of the diffusion coefficient which for a parabolic density profile is given by:

$$D(r) = \frac{a^2}{2r^2 n_o}\int_o^r s(r')r'dr'. \qquad (22)$$

The local ionisation rate, s(r), is given by:

$$s(r) = S(T_e(r))\,N(r)\,n_e(r), \qquad (23)$$

where S is the ionisation rate coefficient, [Lotz, 1967], and N(r) is the neutral density distribution. In practice, the absolute neutral density is difficult to measure. It has been obtained in only a few selected cases in HBTX1B [Evans et al, 1984], but a reliance on using discharge-specific measurements of N(r) would rob the ion power balance modelling of any predictive features. Monte-Carlo simulations of the neutral particle transport show, however, that the relative distribution of neutral density is largely insensitive to the expected experimental range of variation in the $T_e(r)$ and $T_i(r)$ profiles and depends mostly on the n(r) distributions. The calculated N(r) for a parabolic density distribution, together with the experimental values, available from fluorescent scattering, [Evans et al, 1984] are shown in Fig. 3. The computed relative N(r) distribution will be used in Eqns.(23) and (22) to provide the relative D(r) distribution.

To obtain the absolute D(r) on axis we appeal to the axial electron power balance and invoke ambipolar diffusion (i.e. $D_i(0) = D_e(0) = D(0)$). The electron balance of power in the absence of the, generally-small, radiation losses in HBTX1B [Carolan et al, 1987b] is represented by:

$$p_\Omega(r) = \frac{1}{r}\frac{d}{dr}\, r\{G_e(r) + h(r)\}, \tag{24}$$

where $G_e(r)$, the diffusion term, is given by eqn(19), and $h(r)$ represents the thermal conduction term given by:

$$h(r) = f(\frac{\tilde{B}_r}{B})\, K_{||}\, \frac{dT_e}{dr}, \tag{25}$$

where $K_{||}$ is the parallel heat conduction coefficient. The function, $f(\tilde{B}_r/B)$, involving stochastic field line behaviour, is not available for RFP's in a useful form. In the absence of this information we assume for the moment that conduction losses are much less than diffusion losses on axis so that

$$\eta(0)\; j^2(0) \simeq -\frac{1}{r}\frac{d}{dr}\{r\, D\, \frac{d}{dr}\, U_e\}|_{r\to 0}. \tag{26}$$

The possible dominant role of diffusion will be discussed below. In evaluating the r.h.s. of Eqn(26) we express the $n(r)$ and $T_e(r)$ distributions as polynomials of the form:

$$n(r) = n_o\, \{1-\gamma(r/a)^2 + \ldots\}$$

$$T_e(r) = T_{eo}\{1-\delta(r/a)^2 + \ldots\}.$$

Linear terms are suppressed to avoid on-axis discontinuity in the density and temperature gradients. As the axis is approached, only parabolic terms contribute to Eqn(26) so that we get on substitution for $n(r)$ and $T_e(r)$:

$$D(0) \sim \frac{\eta(0)\; j^2(0)\; a^2}{6(\gamma+\delta)\; k\; T_{eo}\; n_o}$$

For a parabolic density profile (γ=1) and a flat electron temperature distribution (δ=0) we obtain:

$$D(0) \sim \frac{\eta(0)\; j^2(0)\; a^2}{6k\; T_{eo}\; n_o}, \tag{27}$$

which on substituting for $\eta(0)$ and $j(0)$ (cf. Eqns (11)-(15)) yields:

$$D(0) \sim \frac{C_1 V_p I_\phi}{12\pi^2 R k T_{eo} n_o}, \qquad (28)$$

where $C_1 = f_1 f_2 f_3^2$; (C_1 is a profile factor for the field and current distributions; it depends primarily on $\lambda(r)$ and therefore on F, θ and β_θ). The value of the diffusion coefficient on axis, given by Eqn (28), is used to normalise the relative D(r) distribution given by Eqn (22). The resulting D(r) distribution for a typical plasma is shown in Fig. 4 where a parabolic density distribution is used in both the Monte-Carlo simulation, to give the relative neutral density distribution, and in the particle balance. Assuming a uniform D(r), spectroscopic measurements on HBTX1B, give $D \sim 100\text{-}150$ $m^2 sec^{-1}$ [Carolan et al, 1987b] (for the same plasma conditions) which is in good agreement with the values shown in Fig 4.

POWER BALANCE OF ELECTRONS

Experimental evidence for a near-flat electron temperature distribution has been reported at ZETA (Rusbridge, 1969), HBTX (Malacarne, 1984), ETA-BETA II (Bassan et al, 1987) and ZT-40M (Wurden et al, 1988). Alternative descriptions of the electron power loss have been suggested by Rusbridge (1969) and Robinson (1975) which may account for these results: (i) The flat electron temperature distribution was attributed by Rusbridge, to the collisional thermal conduction given by Eqn(25). (ii) Robinson, has derived a flat electron temperature distribution by assuming diffusion from turbulent convection.

Our comparison with the experimental data favours the latter description. The effect of diffusion on the ohmically heated electrons is investigated here through the power balance equation, which in the absence of other loss mechanisms (everywhere inside the discharge), has the form:

$$-\frac{1}{r}\frac{d}{dr}\{r\, D(r)\, \frac{d}{dr} U_e(r)\} = \eta(r)\, j^2(r). \qquad (29)$$

At this point it is convenient to introduce the normalised distributions ie: $\bar{D}(x) = D(x)/D(0)$ etc, $(x = r/a)$ so that:

$$-\frac{1}{x}\frac{d}{dx}\{x\,\bar{D}(x)\,\frac{d}{dx}(\bar{n}(x)\,\bar{T}_e(x))\} = \alpha\,(\bar{T}_e(x))^{-3/2}\,\bar{j}^2(x), \qquad (30)$$

where α is the dimensionless parameter:

$$\alpha = \frac{2}{3}\frac{a^2\,\eta(0)\,j^2(0)}{k\,T_{eo}\,n_o\,D(0)}. \qquad (31)$$

For the solution of Eqn(30) we may assume a parabolic density distribution, a parabolic distribution for $j^2(x)$, (which is appropriate for the MBFM), and for $\bar{D}(x)$ the distribution of Fig 4 which can be well represented by the expression: $\bar{D}(x) = 1 + 7x^5$. The solution is subject to the boundary conditions: $\bar{T}_e(x=0) = 1$; $\bar{T}_e(x=1) = 0$; $\frac{d\bar{T}_e}{dx}(x=0) = 0$, and, therefore, Eqn(30) is an eigenvalue equation for α. A numerical solution gives $\alpha \sim 5.5$, corresponding to a near-flat electron temperature distribution but which, steepens near the wall, as shown in Fig 5. A flat temperature distribution can, therefore, be attributed to diffusion losses alone with no need to appeal to collisional thermal conduction. (We may note the value of $\alpha=4$ which follows from substituting Eqn(27), where a flat electron temperature distribution is assumed (i.e. $\delta=0$), into Eqn(31). A different value of $\alpha=5.5$ has been obtained from the analytical solution of the power balance equation because the corresponding electron temperature distribution of Fig. 5 clearly has a second order term with $\delta\neq0$. However, the difference in the calculated values of α is within the present experimental uncertainties in determining $T_e(r)$.)

The value of α (estimated above, giving $\alpha=5.5$) can now be used to estimate the electron temperature on axis. (All of the following formulae are in SI units, apart from temperatures which are in eV's.) We have numerically,

$$\eta(0) = 3.8\ 10^{-5}\ Z_{eff}\ \ln\Lambda\ T_{eo}^{-3/2}\ \gamma_E^{-1}, \qquad (32)$$

where γ_E is the Lorentzian gas correction factor. For the $\lambda(r)$ distribution given by Eqn(8) we get: $j(0) = f_3 I_\phi/\pi a^2$. In this case it can be easily shown from Eqns(31) and (32) that:

$$T_{eo}^{5/2} = 2.6\ 10^{13}\ Z_{eff}\ \ln\Lambda\ \frac{I_\phi^2}{a^2\ n_o\ D(0)\gamma_E}. \qquad (33)$$

Equation (33) may find application in any RFP but for HBTX1B with the following parameters of: a=0.25m, I_ϕ=2.10^{5}A, n_o=3.10^{19}m^{-3}, D(0)=30m^{2}sec^{-1}, Z_{eff}=2.5, we obtain: T_{eo}=210eV which is within the experimental uncertainty of the measured value of T_{eo}=250 ± 40eV. Furthermore, Eqn.(33) reproduces the empirical scaling of the electron temperature with the density and current: $T_{eo} \propto I_\phi^{0.8} n_e^{-0.4}$, [Alper et al, 1987]. Thus, diffusion losses alone can account for (i) the flat electron temperature distribution, (ii) the observed electron temperatures on axis and (iii) the empirical scaling of the electron temperature with the density and current, provided the diffusion coefficient, D(0), does not sensitively depend on either of these quantaties. These results suggest, that diffusion across the magnetic field may be the dominant power loss mechanism in present RFP's.

ION HEATING AND POWER BALANCE

We suggest that the ion heating is a two stage process: the residual power is coupled to the fluctuations, and the energy of these fluctuations is dissipated into ion heating. Assuming that all of the residual power as shown for example in Fig. 2, is finally transmitted to the ions, [Rusbridge, 1969], we can solve numerically Eqn(21) under the boundary conditions: U(a)=0; dU(0)/dr=0. The solution obtained for the ion temperature distribution is shown in Fig. 6 and compared with the experimental results. We also show the experimental points in the outer part of the plasma obtained from fluorescence scattering, [Forrest et al, 1988] and a curve given by $T_i(r) = T_{io}(1-(r/a)^2)^2$ which gives the best fit to the NPA data from the HBTX1B, [Field, 1988] and the ZT-40M, [Wurden et al, 1988] using a Monte Carlo treatment,

[Hughes and Post, 1978] for the neutral particle transport and the energy spectrum. Spectroscopic observations at ZT-40M also support a peaked ion temperature distribution, [Wurden et al, 1987]. Thus, the model, is in a good agreement with experimental observations in predicting a narrow ion temperature distribution (representing a central hot core of ions). Furthermore, the ion temperature on axis is quantitatively reproduced; we have obtained $T_{io} \sim T_{eo}$ which has been found experimentally at the HBTX1B with the edge tile limiters in position.

We also suggest that the residual power available to drive turbulence by the dynamo process is eventually dissipated by viscous damping of the velocity fluctuations, which thereby heat the ions, and we have shown that this residual power can account for the observed ion temperatures. This reduces the ion heating problem to the two following questions: (i) is all of the dynamo power dissipated into the ions? (ii) is the ion viscosity the only ion heating mechanism?

The dynamo power dissipated resistively to the electrons through the fluctuating currents (associated with the magnetic fluctuations) is:

$$Q_e = \eta \, \tilde{j}^2 \sim \eta \, \left(\frac{1}{\mu_o} \frac{\tilde{B}}{\Lambda_\perp}\right)^2 .$$

This with the typical values: $\tilde{B}/B_o \sim 2\%$, $\Lambda_\perp \sim 2\text{cm}$ gives $Q_e \sim 2.10^{-3} p_f$ which is generally negligible compared with the ohmic power $\eta_s j^2$. As regards the ion heating mechanism, it has been shown by Gimblett (1988) that, assuming a magnetic fluctuation level of 2%, the expected fluid velocity fluctuation level, required to sustain the dynamo electric field, is sufficient to provide all the ion heating through parallel viscous damping of the velocity fluctuations.

NORMALISED CALCULATIONS OF T_{io}/T_{eo} FOR THE MOBILE LIMITER EXPERIMENT

A general formula to provide T_{io}/T_{eo} directly from the operating conditions, can be obtained from Eqn(21) which on axis takes the form:

$$-\frac{1}{r}\frac{d}{dr}\{r\,D(r)\,\frac{d}{dr}\,U_i(r)\}|_{r\to 0} = E_\phi\, j_\phi(0) - \eta(0)\, j_\phi^2(0) \qquad (34)$$

The r.h.s. in Eqn(34), by substitution of Eqns(11)-(15), can be written as:

$$E_\phi\, j_\phi(0) - \eta(0)\, j_\phi^2(0) = \frac{V_p}{2\pi R}\,\frac{I_\phi}{\pi a^2}\,(f_3\,\frac{V_\phi}{V_p} - C_1) \qquad (35)$$

To obtain an expression for the l.h.s. of Eqn(34), at the limit of $r\to 0$ (or $r<<a$), we may use: $D(r) \sim$ constant ($\equiv D(0)$ given by Eqn(28)); $U_i(r) \sim \frac{3}{2}\, n_o k T_{io}(1 - \chi(r/a)^2)$. A polynomial fitting of the solution of Eqn.(21) on axis was used to obtain: $\chi \sim 3.5$; (this value arises from a unity contribution from the parabolic density distribution and a 2.5 contribution from the peaked ion temperature distribution of Fig. 7). The l.h.s. of Eqn(34) can then be written as:

$$-\frac{1}{r}\frac{d}{dr}\{r\,D(r)\,\frac{d}{dr}\,U_i(r)\}|_{r\to 0} = \chi\, C_1\,\frac{T_{io}}{T_{eo}}\,\frac{V_p}{2\pi R}\,\frac{I_\phi}{\pi a^2} \qquad (36)$$

Combining Eqns.(35) and (36) we obtain the general formula:

$$\frac{T_{io}}{T_{eo}} = \frac{1}{\chi}\,(C_2^{-1}\,\frac{V_\phi}{V_p} - 1) \qquad (37)$$

where $C_2 \equiv C_1/f_3 = f_1 f_2 f_3$. The profile factor C_2, like C_1, depends on the magnetic field and current distributions and therefore F, θ, β_θ. In Fig. 7, C_2 is shown as a function of θ for the $\lambda(r)$ distribution of Eqn(8) and $\beta(0)$=0, 3%, 8%. It may be noted that C_2 (unlike the other profile factors) is fairly independent of $\beta(0)$ or θ; (for $\beta(0)$ = 0-8% and $\theta \sim 1.4$: $C_2 \simeq 0.48$) so that T_{io}/T_{eo} depends mostly on the ratio V_ϕ/V_p.

Formula (37) for the typical operating conditions of HBTX1B i.e. $V_\phi \sim 30$ Volts and $V_p \sim 14$ Volts gives: $T_{io}/T_{eo} \sim 1$ as seen experimentally. The formula can also provide a minimum value for T_{io}/T_{eo} associated with a perfect boundary with $\Delta V_\phi = 0$ (i.e. $V_\phi = V_p$). For the non uniform $\lambda(r)$, as given by expression (8), we obtain

$$(T_{io}/T_{eo})_{min} = \chi^{-1}(C_2^{-1} - 1) \sim 0.3 \qquad (38)$$

Ion heating in this case is provided by the minimum dynamo activity required to sustain the configuration in the presence of resistive decay of helicity in the plasma bulk but in the absence of edge helicity dissipation (or loss).

The mobile limiter experiments, [Alper et al, 1988] provides the strongest support to the present model. It was observed on HBTX1B that the loop volts has to be increased to sustain the plasma current when a limiter is inserted into the plasma. The suggested interpretation is that the limiter acts as a helicity sink and leads to an increase in ΔV_ϕ. A greater V_ϕ is then required to replenish the helicity loss, or dissipation, at the boundary. The ion heating, which is assumed to be associated with the anomalous voltage, is thereby enhanced and this is supported by the measured values of T_{io}/T_{eo} [Carolan et al 1987a and 1988]. The experimental values of T_{io}/T_{eo}, are shown in Fig. 8, (at a constant current of ~200kAmps but at different insertion distances of the limiter into the plasma), together with the calculated values from Eqn(37) and the experimental values of V_ϕ. In all of these calculations we assume that any variation to the loop volts arises from ΔV_ϕ with V_p remaining almost constant due to the relatively small changes in T_{eo} and Z_{eff} [Alper et al, 1988 and Carolan et al, 1987b]. Mobile limiter experiments carried out at ZT-40M, [Wurden et al, 1988] support the HBTX1B results.

HIGH θ CONDITIONS

The foregoing calculations of profile averaged quantities assume axisymmetry. However, at elevated θ's ($\theta \gtrsim 1.7$) helical plasmas can be observed and are often accompanied by sawteeth-like behaviour in soft X-rays and T_i and a large increase in magnetic fluctuations, $\tilde{B}$. The

increase in loop voltage is higher than expected from calculations assuming axisymmetry with a consequent reduction in τ_E. For example, in HBTX1B ($I_\phi \sim 200$ kA and edge limiter tiles in position), increasing θ from ~ 1.4 to 1.75 resulted in V_ϕ increasing from $\sim$ 30V to $\sim$ 100V [Tsui and Cunnane, 1988] much greater than the $\sim$ 40V expected for axisymmetric plasmas. The results suggest that it is the greatly increased $\tilde{B}$ rather than increased velocity fluctuations which sustain the RFP configuration in these conditions, with the consequence of greater field line stochasticity and reduced confinement and a smaller increase in ion heating from viscous damping of the fluid velocity fluctuations. However, present RFP's are under-diagnosed to investigate these contentions and although enhanced ion heating has been observed in high θ, current ramped discharges in ZT-40M [Wurden et al, 1988], the present model will not be particularly relevant in these conditions.

RESULTS WITH THE TILE LIMITERS REMOVED

Recent theoretical work on magnetic helicity balance has supported the interpretation that the edge tile limiters (covering 10% of the liner wall at the HBTX1B), may play a significant role in the energy confinement. This was corroborated when the confinement time was improved by 50% after limiter removal [Alper et al, 1988]. Typical values of the main plasma parameters, with and without the limiters at the same density and current are given below:

	With Tiles	Without Tiles
I (kA)	200	200
F	-0.07	-0.07
θ	1.4	1.4
V_ϕ (volts)	30	20
β_θ (%)	9	9
τ_E (ms)	0.22	0.33

We see that β_θ has not changed but V_ϕ has decreased by 50% (after limiter removal), providing improved confinement. It has been

suggested that this change in V_ϕ resulted from the variation of the anomalous voltage ΔV_ϕ which is explained with the alternative prescriptions: (i) Jarboe and Alper, (1987) suggested that most of the helicity dissipation takes place in the outer region, even in the current free space behind the limiters; by removing the limiters, this space is reduced and so also is the helicity dissipation; (ii) Tsui, (1987) has suggested that the edge limiters act as a helicity sink similar to the mobile limiter.

Both of the theories however contend that the edge limiters are responsible for overall global helicity loss so that their removal would reduce ΔV_ϕ and the ion heating. The calculated value for T_{io}/T_{eo}, by Eqn.(37) is 0.55 which is in agreement with experimental results for $I_\phi \sim$ 200kA [Carolan et al, 1988]. However, several features of the no-tiles operation of HBTX1B complicate the interpretation when comparing the predicted scalings of T_{io}/T_{eo} with those found experimentally. The scaling experiments (without the limiters) have shown that T_{io}/T_{eo} does not remain constant but increases with the current as shown in Fig. 9, faster than expected from formula (37). Also, the operating range of I_ϕ was extended, where sustained RFP plasmas were possible at very low currents ($\sim$70 kA). These conditions, together with the high T_e's ($\sim$800 eV) observed, yielded the lowest loop voltages yet recorded in RFP's ($\sim$10V). Greater care in the treatment of the input powers to the electrons and ions is required in these new conditions where the anomalous voltage, Spitzer resistivity and plasma current are all relatively small. For example, when it is assumed that only Spitzer resistivity is involved in electron heating we get an experimental scatter plot as shown in Fig. 10 where we display the electron energy density on axis versus $p_\Omega(0)$ ($\equiv \eta_s j^2(0)$). The intercept of $\sim$1000J/m^3 may be due to an additional non ohmic heating of electrons in the RFP, by a yet unknown effect, which becomes apparent without the limiters at the very low values of the Spitzer voltage and the anomalous voltage ΔV_ϕ. The additional input power required is estimated to be about 1MW/m^3; (alternatively, the electron energy confinement time at the lowest currents may increase to a value of $\tau_{E,e} \sim$ 5 msec which is larger by an order of magnitude than the global energy confinement time).

In Fig. 11 we show the corresponding energy density and input power on axis for the ions. Here the input power, $p_i(0)$, takes account of the minimum extra power required to heat the electrons, i.e. $p_i(0) = p_f(0) - 1MW/m^3$. If the T_i and n_e profiles are similar to those obtaining for cases with the tiles in position, the diffusion coefficient on axis is remaining fairly constant for these data, but about 50% lower than that before tile removal. This is consistent with the observed increase in the global energy confinement time [Alper et al. 1988].

Finally, we show in Fig. 12 the ratio T_{io}/T_{eo} as a function of $p_i(0)/p_e(0)$ where $p_e(0) = p_\Omega(0) + 1MW/m^3$. Unfortunately, the scatter in T_{io}/T_{eo} is quite large, due mainly to the uncertainties in measuring T_{eo} from the Si(Li) detector. The slope of the best linear fit to the data is ~ 0.2 and the slope predicted by the model (provided that the temperature and density distributions have not changed on removal of the edge tiles) is:

$$\frac{p_e(0)}{p_i(0)}\frac{T_{io}}{T_{eo}} = \frac{G_e(0)}{G_i(0)}\frac{U_i(0)}{U_e(0)} = \frac{D(0)U_e(0)}{\chi D(0)U_i(0)}\frac{U_i(0)}{U_e(0)} = \chi^{-1} \sim 0.28$$

Thus, the model predictions and the experimental results are in reasonable agreement, considering the relatively large uncertainty in the experimental data.

CONCLUSIONS

By making a series of simple assumptions on the plasma behaviour in RFPs it is possible to construct an ion power balance model whose predictions tally with many of the observations of ion and electron behaviour, such as increasing T_{io}/T_{eo} with limiter insertion, ion temperature distribution and the scaling of T_{eo} and T_{io} with current, density and loop voltage. These results suggest that the main features of the model are justified, given the present uncertainty of experimental data, namely: (i) that the residual input power, after ohmic heating of the electrons, primarily heats the ions and that (ii) the energy confinement of the electrons and ions are governed by the same physics process. Here we suggest that this process is dominated

by diffusion which we show is at least internally consistent with the experimental data on T_i and T_e profiles and on measurements of the diffusion coefficient. Future testing and developments of the model clearly requires more profile measurements of, for example, n_e, T_e, T_i and $\bar{j}$ and how these vary with different conditions, eg. F and θ. The role of impurities should also be included (eg. preferential heating, ion depletion and Z_{eff}). Much theoretical work is also required, especially regarding the ion heating mechanism, the sharing of the non ohmic input powr between ions and electrons, and the energy and particle transport.

ACKNOWLEDGEMENTS

We are especially indebted to A R Field and H Y W Tsui who were involved in the initial discussions and to M K Bevir and C G Gimblett for many helpful suggestions. We are also thankful to B Alper and R J Hayden who measured the electron temperatures and to D E Evans and P D Wilcock who provided the electron density data.

REFERENCES

Alper B et al, (1987) Proc. 11th Int. Conf. on Plasma Phys. and Controlled Nuclear Fusion (Kyoto, 1986), IAEA, Vienna, 2, 399

Alper B et al, (1988) Plasma Physics and Controlled Fusion 30, 843

Bassan M, Flora F, Guidicotti L, (1987); Proc Int. School of Plasma physics on Pnsics of Mirrors, Reversed Field Pinches and Compact Tori (Varenna) III, 1035

Bunting C A, Carolan P G and Field A R, (1985) Proc. 12th EPS Conf on Controlled Fusion and Plasma Physics (Budapest) I 634

Carolan P G et al, (1985) Proc. 10th Int. Conf. on Plasma Phys. and Controlled Nuclear Fusion (London, 1984), IAEA, Vienna, 2, 449

Carolan P G, Field A R, Lazaros A, Rusbridge M G, H Y W Tsui and Bevir M K, (1987a) Proc 14th EPS Conf on Controlled Fusion and Plasma Physics. (Madrid) II, 469

Carolan P G, Bunting C A, Manley A M and Patel A, (1987b) Proc 14th EPS Conf on Controlled Fusion and Plasma Physics (Madrid) II, 515

Carolan P G, Bunting C A and Field A R, (1988) submitted to Plasma Physics and Controlled Fusion

Evans D A, Forrest M J, Nicholson M G, Burgess D D, Carolan P G and Gohill P, (1984) Rev. of Sci. Instrum. 56, 1012

Field A R, (1988) PhD Thesis, Univ. of London.

Forrest M J, Trotman D L, Bamford R and Lazaros A, (1988) Rev. of Sci. Instrum. 59, 1461

Gee S J, (1988) PhD Thesis, UMIST Manchester

Gimblett C G (1988) Private Communication

Hughes M H and Post D C (1978) J. Comp. Phys. 28, 43

Jarboe T R and Alper B, (1987) Physics of Fluids 30, 1177

Johnston J W, (1981) Plasma Physics 23, 187

Lotz W (1967) Max Planck Institut für Plasma-Physik, Garching, Internal Report No. IPP 1/62 (unpublished)

Malacarne M, (1984); PhD. thesis, Oxford University

Ortolani S, (1983) Proc. Int. School of Plasma Physics on Mirror-Based and Field-Reversed Approaches to Magnetic Fusion (Varenna) II 513

Otolani S, (1984) 'Twenty Years of Plasma Physics' 75, Ed McBamara , World Scientific Publ, Philadephia.

Robinson D C, (1975) Proc. of 3rd Conf. on Pulsed High Beta Plasmas, (Culham) 273

Rusbridge M G, (1969) Plasma Physics 11, 35

Schoffer M J, (1984) Phys. Fluids 27, 2129

Schoenberg K F, Moses R W and Hagenson R L, (1984) Physics of Fluids 27, 1671

Taylor J B (1974) Phys. Rev. Lett. 33, 1139

Tsui H Y W, Newton A A, Rusbridge M G, (1986) Proc. 13th EPS Conf. on Controlled Fusion and Plasma Heating (Schliersee) I 345

Tsui H Y W, (1987) Proc. 14th EPS Conf. on Controlled Fusion and Plasma Physics (Madrid) II 473.

Tsui H Y W and Cunanne J A (1988) Plasma Physics and Controlled Fusion 30, 865

Tsui H Y W and Evans D E, (1988) Proc. 15th EPS Conf. on Controlled Fusion an Plasma Heating (Dubrovnik) II 585

Wurden G A et al, (1987) Proc Int. School of Plasma Physics on Physics of Mirrors, Reversed Field Pinches and Compact Tori (Varenna) II, 159

Wurden G A et al, (1988) Proc 15th EPS Conf on Controlled Fusion and Plasma Heating (Dubrovnik) II, 533

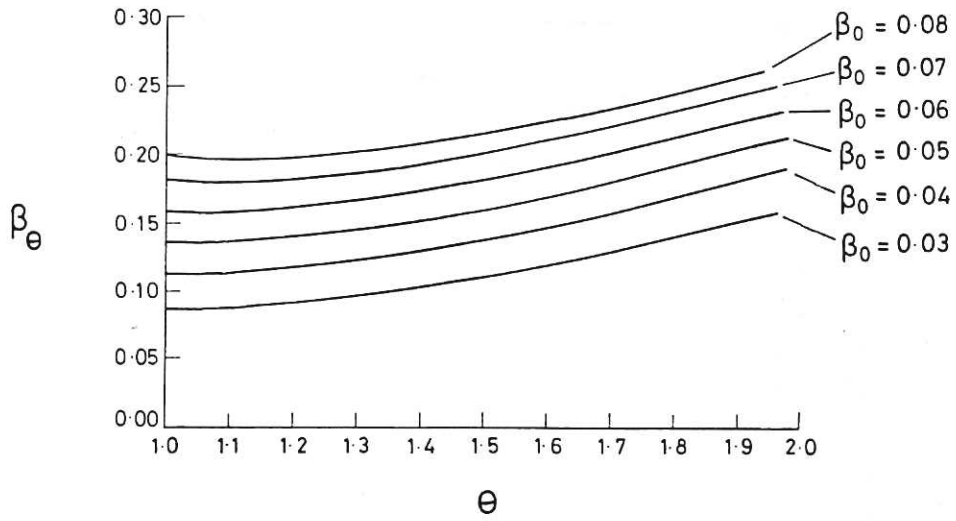

Fig. 1 Calculated β_θ vs θ obtained for $\lambda(r) = \lambda(0)(1-(r/a)^{10})$ and a relative pressure profile of $p(r) = p(0)\{1-(\frac{r}{a})^2\}\{1-(\frac{r}{a})^5\}$

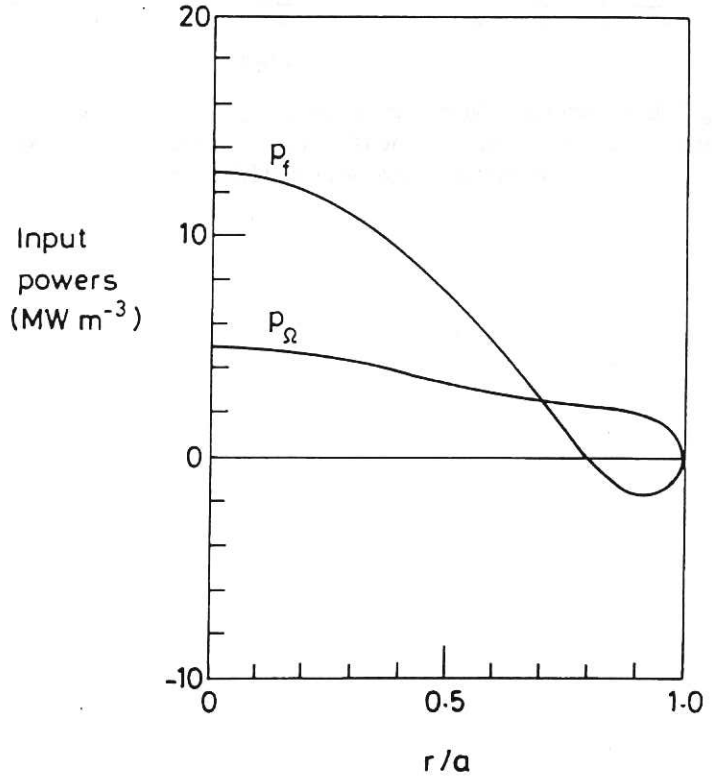

Fig. 2 Power input distributions for the typical operating conditions of HBTX1B (edge tiles in position, centred plasmas, I_ϕ, ~200kA, θ=1.44, F= −0.07, n_{eo}~3×10^{19}m^{-3}).

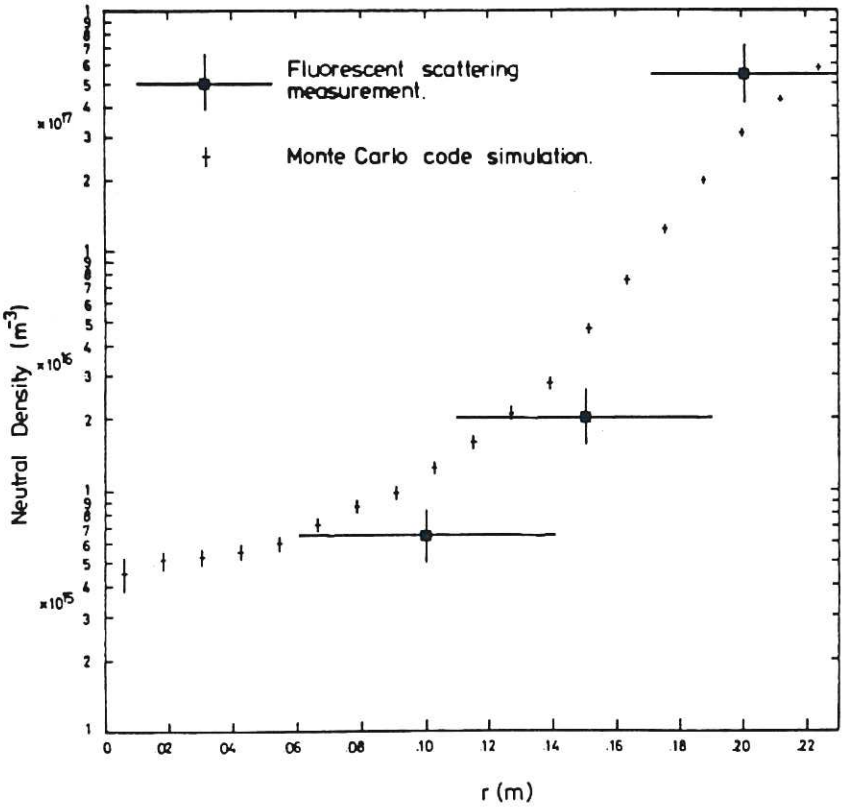

Fig. 3 Experimental (fluorescence scattering) and computed (Monte Carlo simulations) neutral density distributions for the typical operating conditions of HBTX1B.

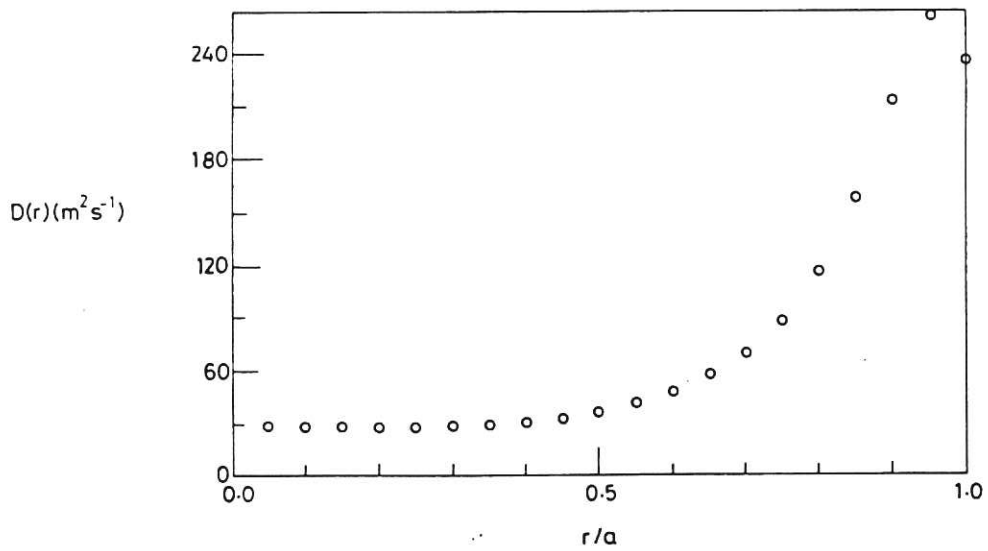

Fig. 4 Calculated deffusion coefficient distribution for the typical operating conditions of HBTX1B.

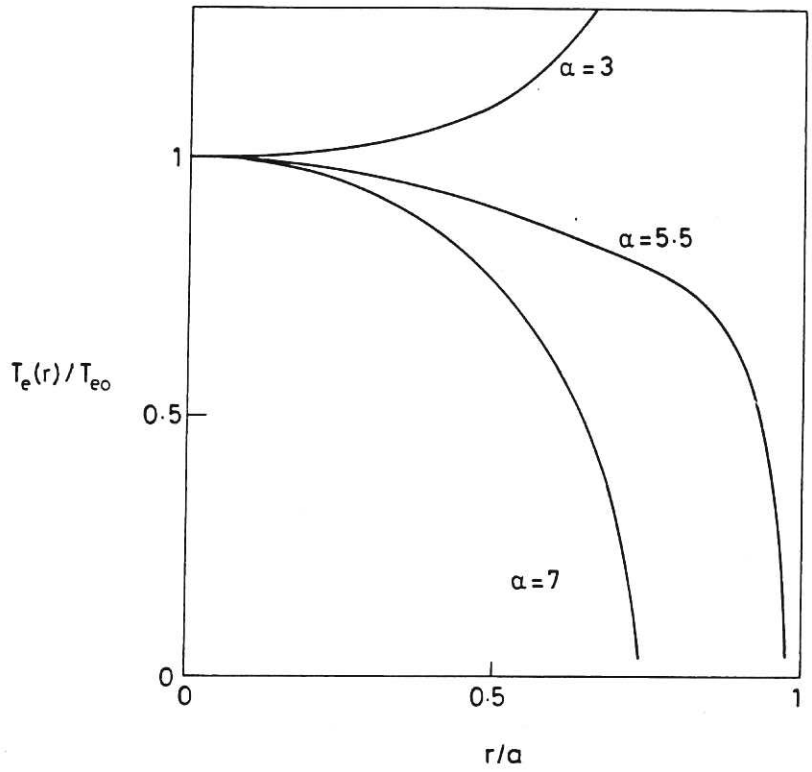

Fig. 5 Parameterised solutions for the normalised electron temperature distribution (cf. Eqn(30)). The physical solution is obtained for $\alpha = 5.5$.

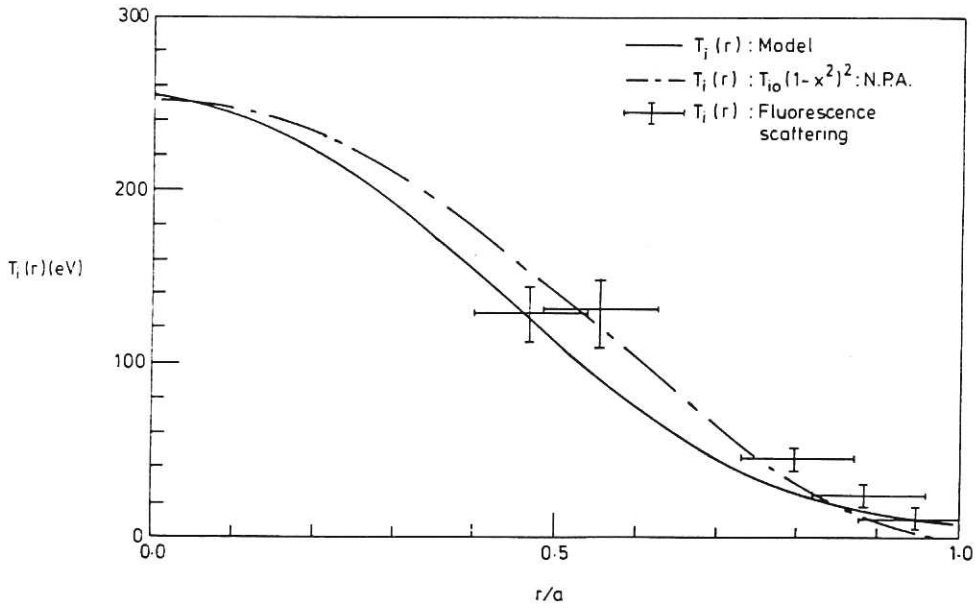

Fig. 6 Experimental (fluorescence scattering and Neutral Particle Analyser) and theoretical (power balance equation) ion temperature distributions for typical operating conditions of HBTX1B.

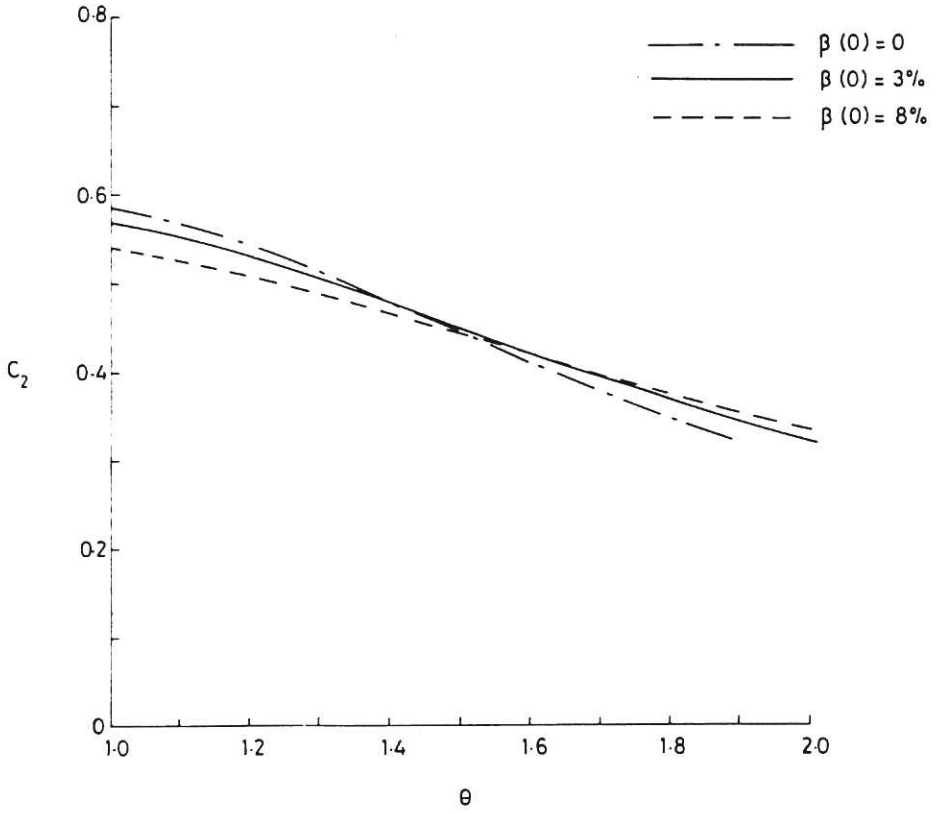

Fig. 7 C_2 vs θ for $\lambda(r) = \lambda(0)\,(1-(r/a)^{10})$ and $\beta(0)=0$, 3%, 8%.

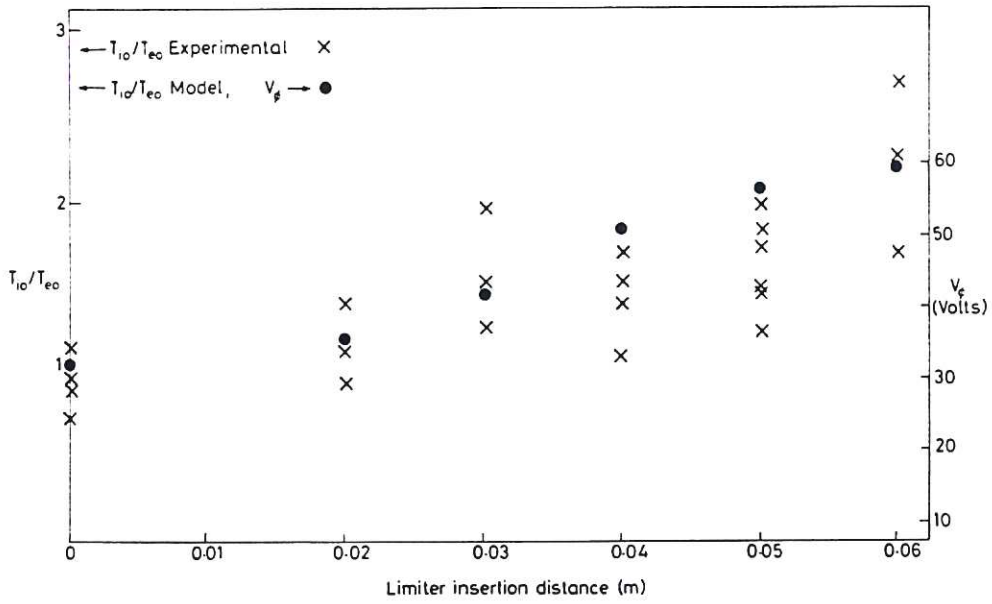

Fig. 8 Experimental and calculated (cf. Eqn (37)) values of T_{io}/T_{eo} versus the insertion distance of a graphite limiter beyond the tiles, together with the corresponding values of V_ϕ.

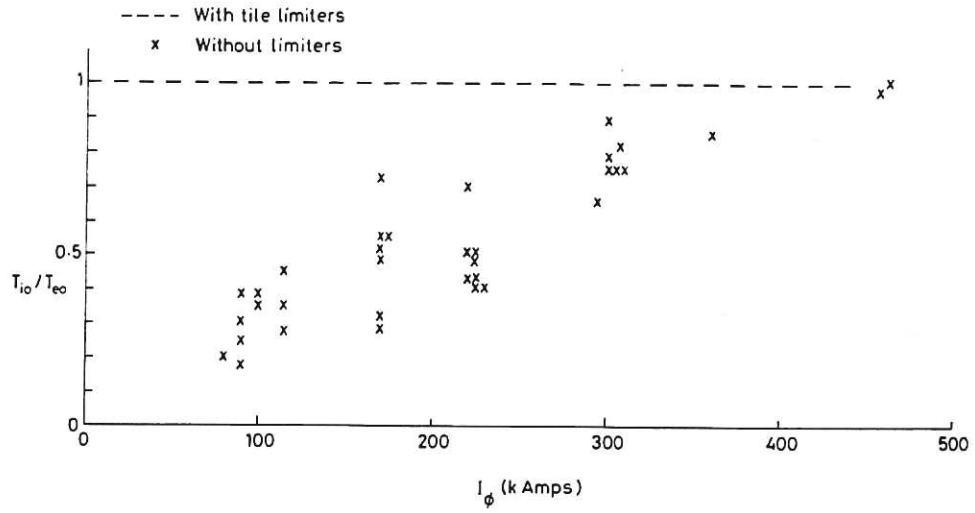

Fig. 9 T_{io}/T_{eo} vs I_ϕ on removal of the edge tiles in HBTX1B.

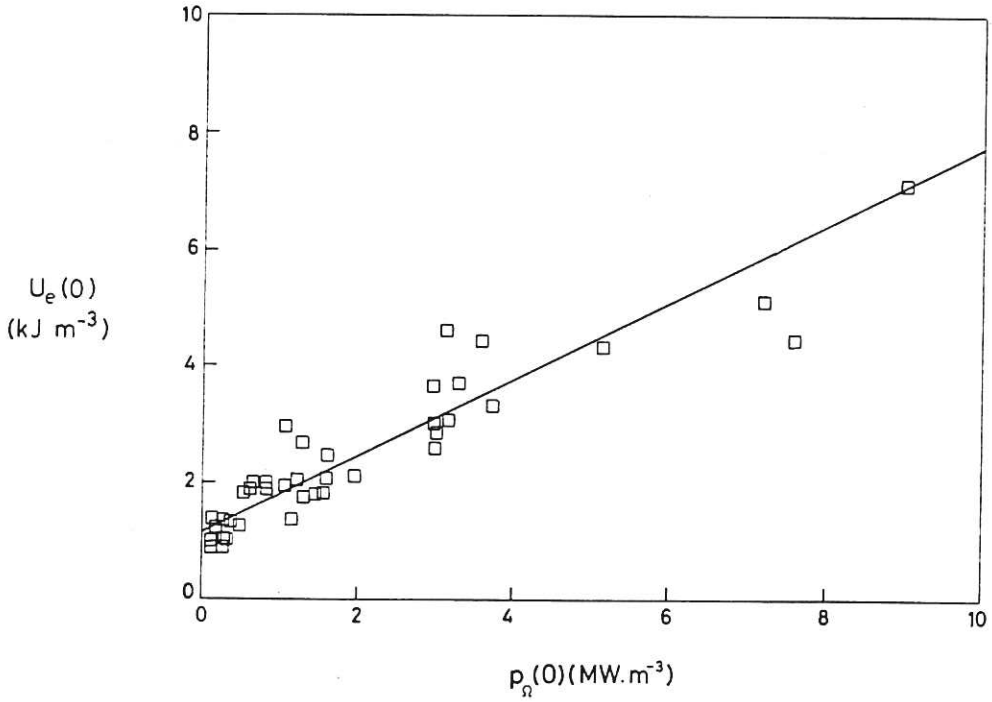

Fig. 10 The electron energy density on axis versus the axial ohmic heating ($p_\Omega(0) = \eta_s j_\phi^2(0)$) for the complete range of currents ($I_\phi \simeq 70$kA-512kA).

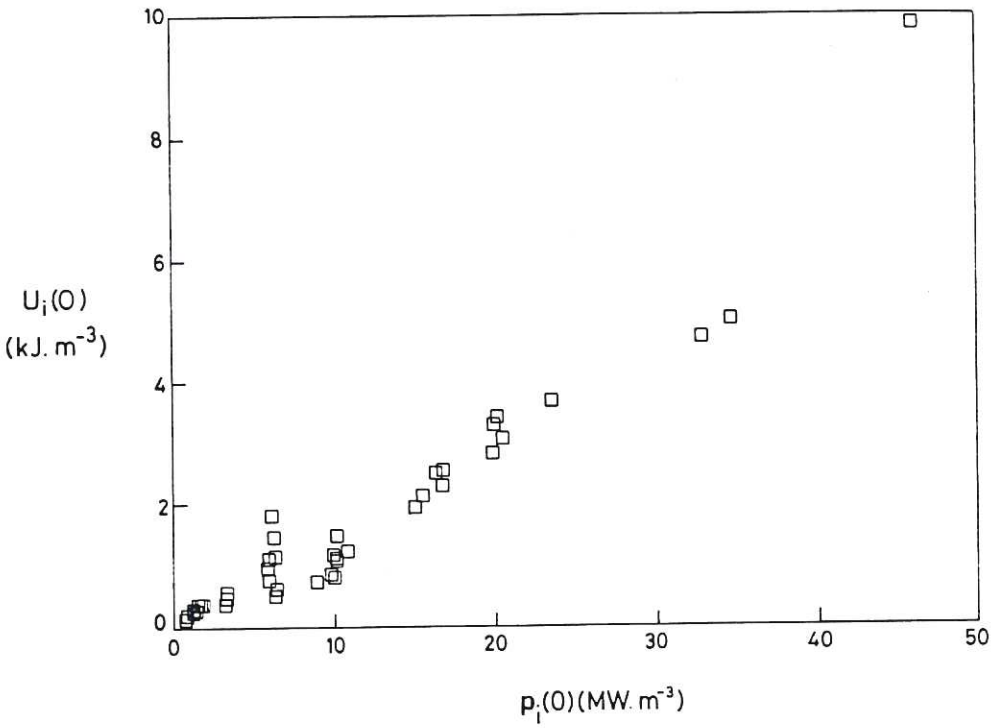

Fig. 11 The ion energy density on axis versus the corrected ion heating rate (i.e. $p_i(0) = E_\omega j_\omega(0) - \eta_s(0) j_\omega^2(0) - 1\,\mathrm{MWm^{-3}}$.)

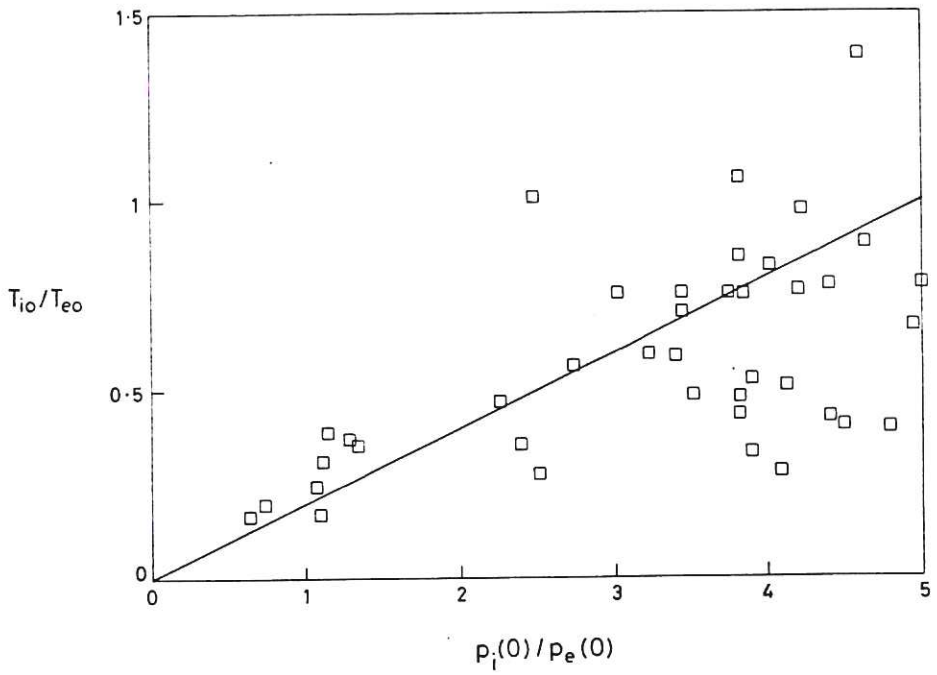

Fig. 12 T_{io}/T_{eo} vs $p_i(0)/p_e(0)$ at the HBTX1B without the edge tiles and including the effect of an additional power input to the electrons of $1\,\mathrm{MWm^{-3}}$ (i.e. $p_e(0) = p_\Omega(0) + 1\,\mathrm{MWm^{-3}}$).